Simple Model for Optical Pulse Propagation in a Reflective Semiconductor Optical Amplifier

M.J. Connelly and C. O'Riordan
Optical Communications Research Group, Dept. Electronic and Computer Engineering, University of Limerick, Limerick, Ireland, E-mail: michael.connelly@ul.ie.

Abstract— **A simple time-domain model is presented that can predict optical pulse propagation in reflective semiconductor optical amplifiers (RSOAs). The RSOA saturation energy, effective lifetime and material gain coefficient parameters used in the model are determined using experimental measurements of the input and output pulse temporal profiles to the RSOA and Levenberg-Marquardt parameter extraction algorithm. The model accurately predicts the propagation of 50.4 ps pulsewidth high-power pulses in the RSOA.**

I. Introduction

The semiconductor optical amplifier (SOA), utilized as an active nonlinear optical medium, has demonstrated its feasibilities in all optical functional applications, such as optical switching and wavelength conversion. Reflective semiconductor optical amplifiers (RSOAs) utilize a high reflective coating on one facet and an anti-reflective coating on the other facet to produce a highly versatile gain medium. Although its waveguide structure is similar to a conventional SOA, RSOAs have a low noise figure and high optical gain at low drive currents. Recently RSOAs have attracted much research interest and found increasing applications in wavelength division multiplexing passive optical networks and in fiber ring mode-locked lasers. [1-3]. It is therefore of interest to model the amplification of optical pulses in RSOA. In this paper we use a simple bidirectional pulse propagation model to predict the propagation of input pulses of 43 ps pulsewidths in a tensile-strained RSOA [4, 5] and incorporate the model in the Levenberg-Marquardt parameter extraction algorithm to extract the RSOA saturation energy, effective lifetime and material gain coefficient parameters.

II. Basic Equations

The RSOA modeled here has the same structure as the device in [4, 5], except that the RSOA has a length of 400 μm and a highly reflective coating applied to the rear facet. The model used is similar to the pulse propagation model described in [6], but uses actual RSOA device parameters obtained using the detailed model [5].

In the slowly-varying envelope approximation, the forward and backward propagating envelopes $A^{\pm}$ of an optical field (where $|A|^2$ is equal to the optical power) in the RSOA can be modeled by

$$\partial A^{\pm}/\partial z \pm v_g^{-1}\,\partial A^{\pm}/\partial t = \mp g(z,t)/2\,(1-j\alpha)A^{\pm} \quad (1)$$

where v_g is the group velocity and α the linewidth enhancement factor. The net gain coefficient g (including the optical confinement factor and internal losses) dynamics can be modeled by

$$\partial g/\partial t = (g_0 - g)/\tau - g\left(\left|A^{+}\right|^2 + \left|A^{-}\right|^2\right)/E_{sat} \quad (2)$$

where g_0 is the unsaturated gain coefficient, τ the effective carrier lifetime and E_{sat} the RSOA saturation energy. In the case of an RSOA with reflectivities of 0 and 1 at the input and reflective ends respectively then the boundary conditions are $A^{+}(0,t) = A_{in}(t)$ and $A^{-}(L,t) = A^{+}(L,t)$, where L is the device length.

III. Numerical Model

In order to obtain a stable numerical solution for (1-2), using the method of [5] we define two independent space-time intervals

$$u = (T+z)/2 \qquad v = (T-z)/2 \quad (3)$$

where the reduced time $T = v_g t$ (units of distance). (3) can be used to transform (1) to

$$\begin{aligned} \partial A^{+}/\partial u &= (g(z,t)/2)(1-j\alpha)A^{+} \\ \partial A^{-}/\partial v &= (g(z,t)/2)(1-j\alpha)A^{-} \end{aligned} \quad (4)$$

The derivatives in (2) and (4) can be approximated by first-order finite differences to give,

$$\begin{aligned} A^{+}(u+\Delta,v) &= A^{+}(u,v) + F_1(u,v)\Delta \\ A^{-}(u,v+\Delta) &= A^{-}(u,v) + F_2(u,v)\Delta \\ g(z,T+\Delta) &= g(z,T) + F_3(z,T)\Delta \end{aligned} \quad (5)$$

978-1-4244-7017-4/10/$26.00 ©2010 IEEE

The step size $\Delta = L/M$ where M is the number of spatial steps (we use a value of 150). Δ is also the step size of the reduced time. $F_{1,2,3}$ is the RHS of (1) and (2). As described in [6], the basic computation procedure is that if the state of the system is known at the reduced time $T = n\Delta$ where n is an integer then at the state of the system for the internal spatial points $(m = 0, M)$ of the system, at $T = (n+1)\Delta$ is given by

$$
\begin{aligned}
&A^{+}(m, N+1) = A^{+}(m, N) + F_1(m-1, N)\Delta; \\
&\qquad\qquad (m \neq 0) \\
&A^{-}(m, N+1) = A^{-}(m+1, N) + F_2(m+1, N); \quad (6) \\
&\qquad\qquad (m \neq M) \\
&g(m, N+1) = g(m, N) + F_3(m, N)\Delta; \quad \forall m
\end{aligned}
$$

The solution of (6) is subject to the boundary conditions described above.

IV. EXPERIMENT AND MODEL VERIFICATION

In our experiment optical pulses, generated using a pulse carving technique whereby an electroabsorption modulator is sinusoidally modulated at 10 GHz by an RF synthesizer, were injected into the RSOA. The input pulse profile is shown in Fig. 1, and has a pulsewidth of 50.4 ps, peak power of 6.9 mW and pulse energy of 0.39 pJ. The input and amplified pulse temporal power profiles were measured using a 65 GHz optical bandwidth digital sampling oscilloscope. The experimentally measured input pulse profile, which was assumed to be chirp free, was used as an actual input into the numerical model. The linewidth enhancement factor used in the model was 2.7, which was determined using the methods described in [7]. E_{sat}, τ and g_0 were determined to be 9.2 pJ, 81 ps and 12.7 x 10^3 m^{-1} respectively by fitting the experimental amplified normalized pulse profile to the model predictions using the Levenberg-Marquardt parameter extraction algorithm. Good agreement between the experimental and modeled output pulse normalized power is shown in Fig. 2. The spatial evolution of the amplified pulse is shown in Fig. 3.

In conclusion, we have developed and experimentally verified the application of a simple model for optical pulse propagation in RSOAs. Further results including a more detailed description of the model, numerical algorithms and more extensive simulations will be presented at the conference.

REFERENCES

[1] E. Wong, Ka Lun Lee and T.B. Anderson, “Directly Modulated Self-Seeding Reflective Semiconductor Optical Amplifiers as Colorless Transmitters in Wavelength Division Multiplexed Passive Optical Networks,” *J. Lightwave Technol*., vol. 25, pp. 67-74, 2007.

[2] W. Zhang, J. Sun, J. Wang, L. Liu, “Multiwavelength modelocked fiber-ring laser based on reflective semiconductor optical amplifiers”, *IEEE Photonics Technol. Lett*., vol. 19, pp. 1418-1420, Oct. 2007.

[3] L. Q. Guo and M. J. Connelly, "A novel approach to all-optical wavelength conversion by utilizing a reflective semiconductor optical amplifier in a co-propagation scheme." *Optics Comms*, vol. 281, no. 17, pp. 4470-4473, 2008.

[4] C. Michie, A. E. Kelly, J. McGeough, I. Armstrong, and I. Andonovic, ”Polarization-Insensitive SOAs Using Strained Bulk Active Regions,” *J. Lightwave Technol*., vol. 24, pp. 3920-2006.

[5] M. J. Connelly, “Wide-band Steady-State Numerical Model and Parameter Extraction of a Tensile-Strained Bulk Semiconductor Optical Amplifier,” *IEEE J. Quantum Electron*., vol, 43, pp. 47-56, 2007.

[6] Jacques W. D. Chi, L. C., and M. K. Rao, "Time-Domain Large-Signal Investigation on Nonlinear Interactions Between An Optical Pulse and Semiconductor Waveguides", *IEEE J. Quantum Electron.,* vol. 37, no. 10, pp. 1329-1336, 2001.

[7] M. J. Connelly, "Theoretical calculations of the carrier induced refractive index change in tensile-strained InGaAsP for use in 1550 nm semiconductor optical amplifiers." *Appl. Phy. Lett*., vol. 98, no. 11, pp. 181111-3, 2008.

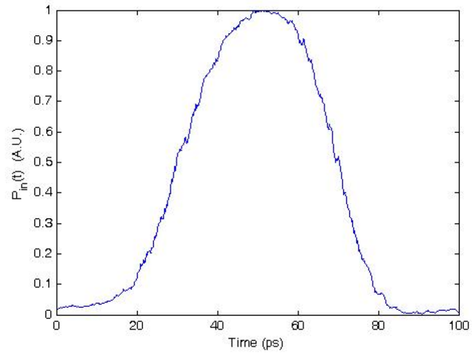

Fig. 1. Input pulse power profile.

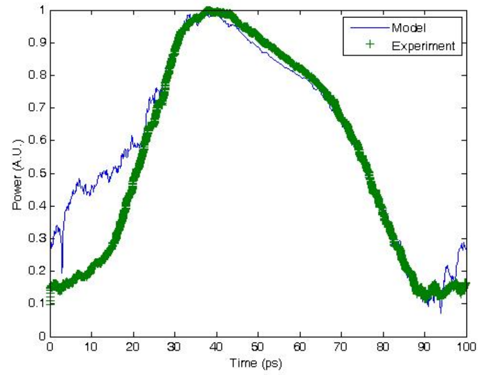

Fig. 2. Experimental and modeled output pulse power.

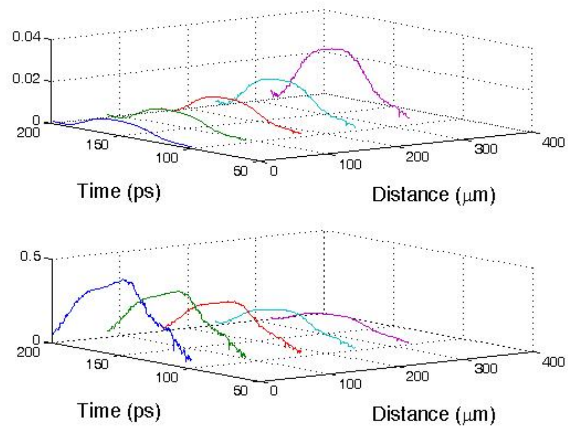

Fig. 3. Spatial evolution of the forward (top) and reflected (bottom) amplified pulse in an RSOA.